Mon. Not. R. Astron. Soc. **000**, 1–5 (1996) Printed 1 February 2008 (MN LATEX style file v1.4)

The Las Campanas Redshift Survey Galaxy-Galaxy Autocorrelation Function

D. L. Tucker,[1,2] A. Oemler, Jr.,[3,4] R. P. Kirshner,[5] H. Lin,[6] S. A. Shectman,[3] S. D. Landy,[3] P. L. Schechter,[7] V. Müller,[2] S. Gottlöber,[2] and J. Einasto[8]

[1] *Fermilab, MS 127, P.O. Box 500, Batavia, IL 60510 USA*
[2] *Astrophysikalisches Institut Potsdam, An der Sternwarte 16, D-14482 Potsdam, Germany*
[3] *Carnegie Observatories, 813 Santa Barbara Street, Pasadena, CA 91101 USA*
[4] *Dept. of Astronomy, Yale University, New Haven, CT 06520-8101 USA*
[5] *Harvard-Smithsonian Center for Astrophysics, 60 Garden Street, Cambridge, MA 02138 USA*
[6] *Dept. of Astronomy, University of Toronto, 60 St. George St., Toronto, ONT M5S 3H8, Canada*
[7] *Dept. of Physics 6-214, Massachusetts Institute of Technology, Cambridge, MA 02139 USA*
[8] *Tartu Astrophysical Observatory, EE-2444 Toravere, Estonia*

Accepted 1996 November 10. Received 1996 August 1

ABSTRACT

Presented are measurements of the observed redshift-space galaxy-galaxy autocorrelation function, $\xi_{\rm gg}(s)$, for the Las Campanas Redshift Survey (LCRS). For separations $2.0h^{-1}$ Mpc $< s < 16.4h^{-1}$ Mpc, $\xi_{\rm gg}(s)$ can be approximated by a power law with slope $\gamma = -1.52\pm0.03$ and correlation length $s_0 = 6.28\pm0.27h^{-1}$ Mpc. A zero-crossing occurs on scales of $\sim 30-40h^{-1}$ Mpc. On larger scales, $\xi_{\rm gg}(s)$ fluctuates closely about zero, indicating a high level of uniformity in the galaxy distribution on these scales. In addition, two aspects of the LCRS selection criteria – a variable field-to-field galaxy sampling rate and a 55 arcsec galaxy pair separation limit – are tested and found to have little impact on the measurement of $\xi_{\rm gg}(s)$. Finally, the LCRS $\xi_{\rm gg}(s)$ is compared with those from numerical simulations; it is concluded that, although the LCRS $\xi_{\rm gg}(s)$ does not discriminate sharply among modern cosmological models, redshift-space distortions in the LCRS $\xi_{\rm gg}(s)$ will likely provide a strong test of theory.

Key words: cosmology: observations – large-scale structure of the universe – galaxies: clustering – surveys

1 INTRODUCTION

The original goals of the Las Campanas Redshift Survey (LCRS; Shectman et al. 1996) were two-fold: firstly, to attempt to sample a 'fair and typical' volume of the nearby Universe in order to constrain the size of the largest structures in the local galaxy distribution, and, secondly, to use this sample to study galaxy clustering on a wide variety of scales. In order to accomplish these goals, it was decided that the survey should be both spatially deep and angularly wide. Indeed, the LCRS fulfills both these criteria in that it extends to a redshift of ~ 0.2 and it is composed of a total of 6 alternating $1.^{\circ}5 \times 80^{\circ}$ slices – 3 each in the North and South Galactic Caps. A visual inspection of the slices indicates that the largest walls and voids have sizes of $50-100h^{-1}$ Mpc, much smaller than the largest survey dimensions, suggesting that the LCRS does in fact encompass a fair sample. Clearly, such data provide exemplary material for the study of large-scale galaxy clustering.

Recently completed, the LCRS now contains 26,418 galaxy redshifts, 23,697 of which lie within the survey's official geometric and photometric borders. Accurate sky positions and Kron-Cousins R-band photometry have come from CCD drift scans at the Las Campanas Swope 1-m telescope; spectra have been obtained at the Las Campanas Du Pont 2.5-m telescope, originally with a 50-fibre Multi-Object Spectrograph (MOS) and later with a 112-fibre MOS. For observing efficiency, all the fibres are used, but each MOS field is observed only once. Hence, the LCRS is a collection of 50-fibre fields (with nominal apparent magnitude limits of $16.0 \leq R < 17.3$) and 112-fibre fields (with nominal apparent magnitude limits of $15.0 \leq R < 17.7$). Thus, selection criteria vary from field to field, but they are carefully documented and are therefore easily taken into account. Observing each field only once, however, creates an additional selection effect: the individual fibres' protective tubing prevents the observation of galaxy pairs within 55 arcsec of each other. Hence, the cores of rich clusters may be undersampled, potentially causing underestimates

in measurements of small-scale galaxy clustering. In this paper, we will consider the LCRS redshift-space galaxy-galaxy autocorrelation function, $\xi_{\rm gg}(s)$. We will also examine the influence on it from the fibre-separation limit and the field-to-field sampling variations. Finally, we will compare the LCRS $\xi_{\rm gg}(s)$ with those derived from numerical simulations.

2 METHOD

To account for the survey geometry and for the field-to-field variations in the nominal apparent magnitude limits and in the sampling fraction, we generate catalogues of random galaxies over the same survey volume with the same field-to-field characteristics as the observed LCRS catalogue. (Note that, although its inclusion would tend to diminish the effects of undersampling on small scales, for ease of interpretation the fibre-separation limit is *not* implemented into the random catalogues.) The redshift distribution of random galaxies is determined via the LCRS luminosity function described in Lin et al. (1996a), incorporating the subtleties detailed in Section 3.2 of that paper. We then calculate $\xi_{\rm gg}(s)$ according to the Hamilton (1993) formalism,

$$1+\xi_{\rm gg}(s) = \frac{RR(s)}{DR(s)} \times \frac{DD(s)}{DR(s)}, \tag{1}$$

where $DD(s)$, $DR(s)$, and $RR(s)$ are, respectively, the weighted data-data pair count ($\Sigma_{i\neq j} w_i w_j$), the weighted data-random pair count ($\Sigma w_i w_j^{\rm r}$), and the weighted random-random pair count ($\Sigma_{i\neq j} w_i^{\rm r} w_j^{\rm r}$) for the (comoving) separation s; RR/DR is a measure of the relative mean density of galaxies in the observed and random catalogues. Aside from small differences in the large-scale normalisation, our results change little if a classic Davis & Peebles (1983) approach is employed (see Fig. 1 below). We prefer the Hamilton formalism, however, since it is less affected by uncertainties in the mean density of galaxies (see also Landy & Szalay 1993).

For the pair counts, Hamilton (1993) suggests the minimum variance weight for each galaxy,

$$w_i = \frac{1}{1+4\pi n_{\rm fld}^{\rm exp}(z_i) J_3(s)} \tag{2}$$

(likewise for $w_i^{\rm r}$), where $n_{\rm fld}^{\rm exp}(z_i)$ is the number density of galaxies one would expect to observe at a redshift z_i for a given field under the constraints of the luminosity function and of the selection effects peculiar to that field, and where

$$J_3(s) \equiv \int_0^s x^2 \xi(x) dx. \tag{3}$$

For this integral, we have approximated ξ by a power law with slope -1.6 and correlation length $s_0 = 6.0h^{-1}$ Mpc, which is a good approximation for separations $2h^{-1}$ Mpc $\lesssim s \lesssim 20h^{-1}$ Mpc (see Sec. 3.1). Results are robust for reasonable values of the slope and correlation length.

Due to the typical distances involved, galaxy velocities are corrected for CMB-dipole motion (Lineweaver et al. 1996) rather than for a Virgo infall model; tests indicate, however, that simply using heliocentric velocities has little effect on the analysis. Positions are then converted into comoving distances assuming $H_0 = 100h$ km s^{-1} Mpc^{-1}, $q_0 = 0.5$, and $\Lambda = 0$. In order to avoid the weights 'blowing up' at the survey's extremal distances, we confine our analysis of $\xi_{\rm gg}(s)$ to those galaxies in the LCRS with velocities of $10,000$ km s^{-1} $\leq cz_{\rm CMB} \leq 45,000$ km s^{-1} and with R-band absolute magnitudes of $-22.50 \leq M_R - 5\log h \leq -18.50$; 19,314 galaxies from the official LCRS sample meet these criteria. The random catalogues typically contain a similar number of galaxies.

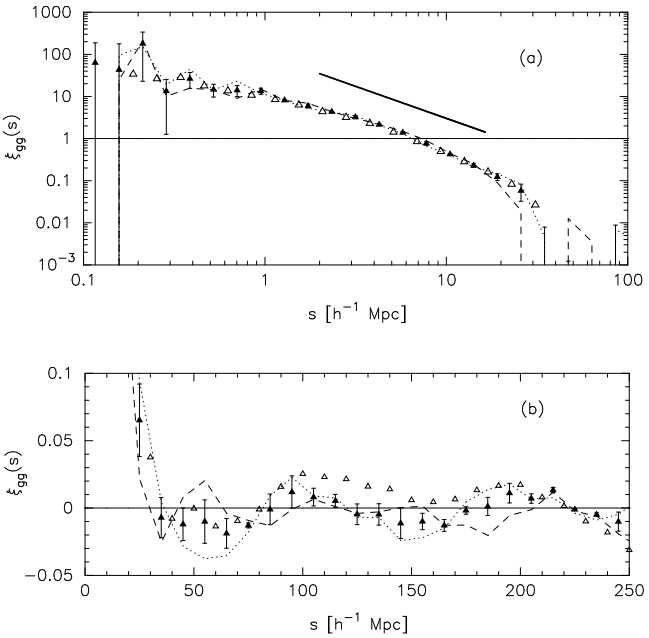

Figure 1. The observed LCRS $\xi_{\rm gg}(s)$ for (a) small-to-intermediate scales and for (b) intermediate-to-large scales. The *filled triangles* denote $\xi_{\rm gg}(s)$ for the combined North and South Galactic Cap sample, the *dashed line* for the Northern Cap sample alone, and the *dotted line* for the Southern Cap sample alone; these measurements all use the Hamilton formalism. For comparison, the LCRS $\xi_{\rm gg}(s)$ calculated using the Davis & Peebles formalism is also presented (*unfilled triangles*); here, as with the Hamilton formalism, the weighting scheme of equation (2) is employed. For clarity, only the *filled triangles* show error bars. Finally, a -1.52 power law, offset, is shown in (a) for the interval $2.0h^{-1}$ Mpc $< s < 16.4h^{-1}$ Mpc (*thick solid line*).

In what follows, 1σ error bars are estimated by calculating $\xi_{\rm gg}(s)$ in independent subregions of the LCRS and taking the standard deviation of the mean. For $s \leq 200h^{-1}$ Mpc, the LCRS is split into four separate subregions (Northern Galactic Cap data, RA $\leq 12^{\rm h}\ 42^{\rm m}$ and RA $> 12^{\rm h}\ 42^{\rm m}$; Southern Galactic Cap, RA $\leq 00^{\rm h}\ 42^{\rm m}$ and RA $> 00^{\rm h}\ 42^{\rm m}$). For $s > 200h^{-1}$ Mpc, only two independent subregions are considered – the Northern Galactic Cap and the Southern Galactic Cap survey volumes. [Note: preliminary tests indicate that, for our sample, the bootstrap errors (Ling, Frenk, & Barrow 1986) are comparable in magnitude to those calculated with the above method.]

3 RESULTS

3.1 The Observed LCRS $\xi_{\rm gg}(s)$

The results for the observed LCRS $\xi_{\rm gg}(s)$ can be found in Figure 1. For separations $2.0h^{-1}$ Mpc $< s < 16.4h^{-1}$ Mpc, we find that the observed LCRS $\xi_{\rm gg}(s)$ can be approximated by a power law with slope $\gamma = -1.52 \pm 0.03$ and correlation

length $s_0 = 6.28 \pm 0.27h^{-1}$ Mpc (Fig. 1a, Hamilton formalism). A zero-crossing occurs at $s \sim 30 - 40h^{-1}$ Mpc. On larger scales, $\xi_{gg}(s)$ fluctuates closely about zero, evidence of a high level of uniformity in the galaxy distribution on these scales (Fig. 1b). Although possible small-amplitude ($\delta\xi_{gg} \approx 0.01 \pm 0.01$) secondary maxima do appear at $\sim 100h^{-1}$ Mpc and at $\sim 200h^{-1}$ Mpc, whether these (and other, larger-scale) relative extrema are characteristic of the galaxy distribution itself or merely statistical fluctuations within the sampled volume remains a matter of debate and is still under investigation. It is interesting to note, however, that these large-scale features – and the differences between the LCRS North and South Galactic Cap samples – are reflected in Landy et al. (1996)'s determination of the LCRS 2D power spectrum (their Fig. 2), and that Doroshkevich et al. (1997)'s core-sampling analysis of the LCRS reveals a scale of $\sim 100h^{-1}$ Mpc for the typical separation of sheet- or wall-like structures. Furthermore, in an independent sample, Einasto et al. (1997) find similar features in the autocorrelation function for clusters in the environments of rich superclusters.

Finally, we compare the LCRS $\xi_{gg}(s)$ with those from two other modern redshift surveys (Fig. 2): Park et al.'s (1994) determination for a sample of the extended CfA Redshift Survey (CfA2) and Loveday et al.'s (1996) determination for the Stromlo-APM Redshift Survey. The Park et al. sample under discussion covers 2 sr of sky out to a comoving depth of $101h^{-1}$ Mpc and consists of 7453 galaxies with $m_{B(0)} \leq 15.5$ (their CfA101m sample). The Stromlo-APM Redshift Survey, the basis of the Loveday et al. analysis, covers 1.3 sr of sky and contains 1787 galaxies with $b_J \leq 17.15$ which were randomly selected at a rate of 1 in 20 from the APM galaxy catalogue (Maddox et al. 1990). The autocorrelation functions from both these surveys match the LCRS $\xi_{gg}(s)$ quite well on small scales ($s \lesssim 10h^{-1}$ Mpc). Unfortunately, the CfA2 $\xi_{gg}(s)$, calculated using the Davis & Peebles formalism becomes unreliable on scales $s \gtrsim 15h^{-1}$ Mpc, due to the fractional uncertainty in the mean number density of galaxies (Park et al. 1994). On the other hand, the Stromlo-APM $\xi_{gg}(s)$, calculated via the Hamilton formalism, is less hampered by uncertainties in the mean galaxy number density; that it appears to show some excess power relative to the LCRS $\xi_{gg}(s)$ on large scales ($s \gtrsim 20 - 30h^{-1}$ Mpc) may indicate real differences in the clustering properties of the LCRS and the Stromlo-APM samples.

3.2 The Fibre Separation Test

To test the effects of fibre separation, we have artificially increased the fibre separation criterion in each MOS field from the original 55 arcsec – first to 90 arcsec and then to 120 arcsec. This was done by culling the original LCRS catalogue – field-by-field – of one galaxy in any pair separated on the sky by less than the artificial fibre limit. We can then extrapolate backwards to estimate how the original 55 arcsec separation limit affects the measurement of $\xi_{gg}(s)$. For a more direct test, we have also taken 5 individual mock slices – each based upon the Standard Cold Dark Matter (SCDM) simulations of Section 3.4 – and then imposed a 55 arcsec fibre separation limit in a manner akin to that for a real LCRS slice.

The effect is negligible on all but the smallest scales, $s \lesssim 1h^{-1}$ Mpc (Fig. 3). At these scales, however, Poisson errors begin to dominate the results, making it difficult to assess the exact magnitude of the effect. Nonetheless, even at separations of $s \sim 0.3h^{-1}$ Mpc, it appears that the LCRS 55 arcsec fibre separation limit results only in a $\sim 10 - 20$ per cent underestimate of the 'true' $\xi_{gg}(s)$. On scales of $1h^{-1}$ Mpc $\lesssim s \lesssim 20h^{-1}$ Mpc, measurements of $\xi_{gg}(s)$ are depressed typically by $\lesssim 5$ per cent due to fibre separation, and, on the largest scales (Fig. 3b), the fibre separation effect is hardly evident.

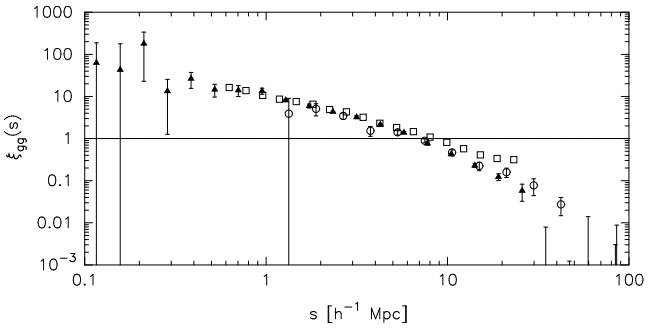

Figure 2. A comparison of the LCRS $\xi_{gg}(s)$ (Hamilton formalism) from Fig. 1 (*filled triangles*) with determinations from two other optically selected modern surveys: Park et al.'s (1994) minimum variance estimate of $\xi_{gg}(s)$ (Davis & Peebles formalism) for the CfA Redshift Survey (*unfilled squares, no error bars available*) and Loveday et al.'s (1996) minimum variance estimate of $\xi_{gg}(s)$ (Hamilton formalism) for the Stromlo-APM Redshift Survey (*unfilled circles with error bars*).

3.3 The Uniform Sampling Test

Although the variations in the field-to-field sampling are included both in the random catalogue of galaxies and in the galaxy weighting [equation (2)], there may be concern that these variations may still result in some residual aliasing of power in the observed $\xi_{gg}(s)$ [this would be in addition to any aliasing due to the slice geometry of the Survey; cf. Kaiser & Peacock (1991)]. Therefore, to test the effects of the field-to-field variations in the nominal apparent magnitude limits and in the sampling fraction, two uniform galaxy catalogues were extracted from the LCRS: a catalogue of uniform field sampling fraction (21 per cent, the most restrictive in the LCRS) and of uniform apparent magnitude limits ($16.33 \leq R < 17.13$) was extracted from the full 50- & 112-fibre LCRS. This uniform catalogue (the uLCRS) contains $\sim 1/7$ the number of galaxies from the original catalogue. A second uniform catalogue (containing $\sim 1/3$ the number galaxies of the original) was extracted from just the set of 112-fibre fields. This catalogue (the uLCRS112) has a uniform field sampling fraction of 34 per cent (the most restrictive from the 112-fibre fields) and uniform apparent magnitude limits, $15.18 \leq R < 17.47$.

Owing to the greater statistical noise of the two uniform catalogues (due to their greatly truncated samples), it is hard to distinguish any significant difference between the $\xi_{gg}(s)$ derived from the full LCRS sample and those from the uLCRS and the uLCRS112 (Fig. 4). Indeed, on small-to-intermediate scales (Fig. 4a), any effect must be of a mag-

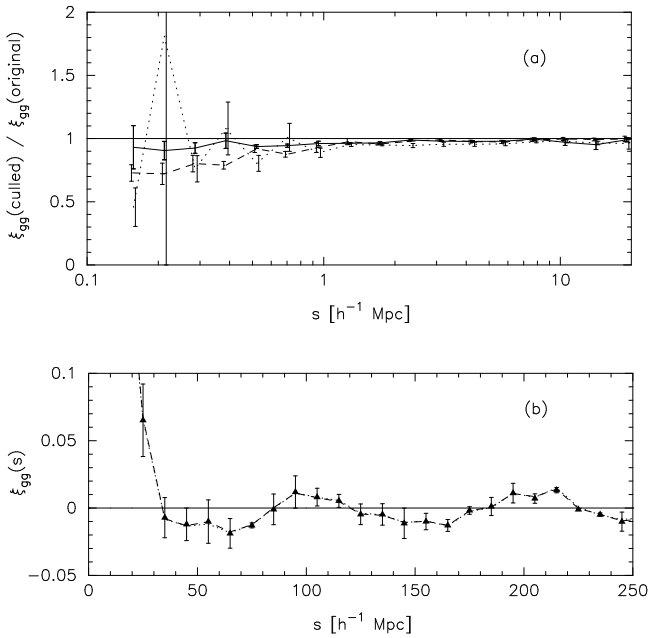

Figure 3. The Fibre Separation Test. (a) On small-to-intermediate scales we plot the ratio of $\xi_{\rm gg}(s)$ of a catalogue culled to a given fibre separation limit to that of the original catalogue, $\xi_{\rm gg}$(culled)/$\xi_{\rm gg}$(original). This ratio is plotted only on those scales where both $\xi_{\rm gg}$(culled) and $\xi_{\rm gg}$(original) are clearly positive. For the LCRS data, $\xi_{\rm gg}$(original) is the LCRS $\xi_{\rm gg}(s)$ from Fig. 1a (Hamilton formalism); we plot this ratio for the LCRS catalogue culled to 90 arcsec (*dashed line*) and to 120 arcsec (*dotted line*) fibre separation limits. Error bars are the standard deviation of the mean of $\xi_{\rm gg}$(culled)/$\xi_{\rm gg}$(original) from the same four subvolumes used to calculate the error in the LCRS $\xi_{\rm gg}(s)$ on these scales. For the SCDM mock slices, $\xi_{\rm gg}$(original) is $\xi_{\rm gg}(s)$ with no fibre separation limit; $\xi_{\rm gg}$(culled) is $\xi_{\rm gg}(s)$ for the mock slice culled to a fibre separation limit of 55 arcsec. We plot the mean of this ratio based upon 5 individual mock slices (*solid line*), where the error bars are the standard deviation of the mean. (b) On intermediate-to-large scales, we simply plot $\xi_{\rm gg}(s)$: the *filled triangles* are as in Fig. 1, the *dashed line* is the LCRS $\xi_{\rm gg}(s)$ with a 90 arcsec fibre separation limit, and the *dotted line* is the LCRS $\xi_{\rm gg}(s)$ with a 120 arcsec fibre separation limit.

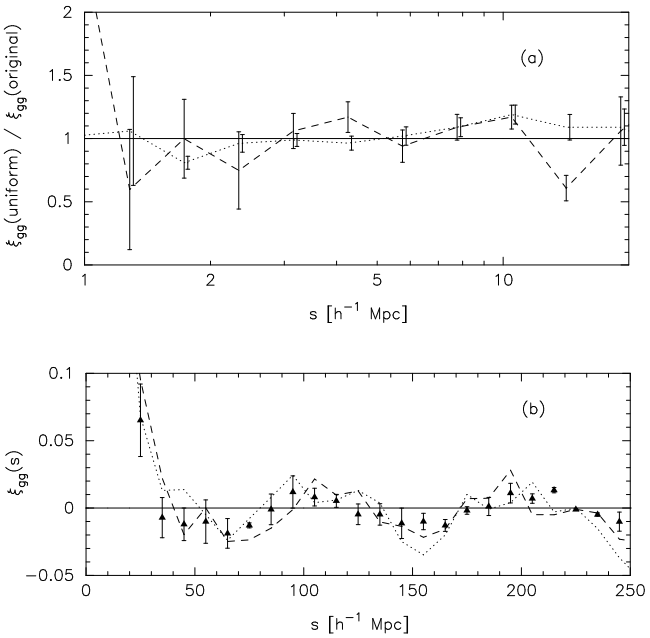

Figure 4. The Uniform Sampling Test. (a) On small-to-intermediate scales we plot the ratio of $\xi_{\rm gg}$ for the LCRS catalogue culled to uniform sampling to $\xi_{\rm gg}(s)$ for the full LCRS catalogue (such as in Fig. 1). This ratio is plotted only on those scales where $\xi_{\rm gg}(s)$ is clearly positive for both the original and the uniform catalogues. The (*dashed line*) denotes the ratio for the uLCRS catalogue, and the (*dotted line*) for the uLCRS112 catalogue. Error bars are the standard deviation of the mean of $\xi_{\rm gg}$(uniform)/$\xi_{\rm gg}$(original) from the same four subvolumes used to calculate the error in the LCRS $\xi_{\rm gg}(s)$ on these scales. (b) On intermediate-to-large scales, the *filled triangles* are as in Fig. 1, the *dashed line* denotes the $\xi_{\rm gg}(s)$ from the uniformly sampled uLCRS catalogue, and the *dotted line* denotes the $\xi_{\rm gg}(s)$ from the uniformly sampled uLCRS112 catalogue.

nitude of $\lesssim 20$ per cent; on large scales (Fig. 4b), any effect must be of amplitude $\delta\xi_{\rm gg} \lesssim 0.01$. The present analysis is consistent with the null hypothesis that the LCRS $\xi_{\rm gg}(s)$, as calculated, does *not* suffer from aliasing due to field-to-field sampling variations. The placement of more stringent limits on this effect will require extensive testing with mock catalogues covering the full LCRS volume.

3.4 Comparison with Theory

For this study, galaxy catalogues for three cosmological models were produced – one based on the Standard Cold Dark Matter (SCDM) model ($H_0 = 50$ km s^{-1} Mpc^{-1}, $\Omega_0 = 1$), another on a non-zero cosmological constant model (ΛCDM; $H_0 = 70$ km s^{-1} Mpc^{-1}, $\Omega_0 = 0.35$, $\Omega_\Lambda = 0.65$), and a third on the Broken Scale Invariance (BSI) model predicted by a double–inflation scenario (Gottlöber, Müller, & Starobinsky 1991; Gottlöber, Mücket, & Starobinsky 1994). All models are COBE normalised. We have studied structure formation in $200h^{-1}$ Mpc and $150h^{-1}$ Mpc boxes for the SCDM/BSI and the ΛCDM simulations, respectively, using a PM code with 128^3 particles in 256^3 grid cells (Kates et al. 1995).

Galaxies are identified as local maxima in the density field of dark matter, with an overdensity of 30 for the BSI and ΛCDM simulations and an overdensity of 70 for the more evolved SCDM. These thresholds are a compromise between the results of spherical collapse estimates and the low spatial resolution of the simulation. Then we collected all the particles into 'halos' with a diameter of a grid cell length and produced a random realisation of the LCRS luminosity function. To this end, we used mass-to-light ratios of $M/L = 80$, 150, and 240 for the ΛCDM, BSI, and SCDM simulations, respectively, in order to provide the total luminosity predicted by the integrated LCRS luminosity function for the summed masses of the peak-selected halos. Further, we distributed the 'galaxies' within the volume of the halo with a Gaussian spatial displacement and with a Gaussian velocity dispersion with a variance according to the virial theorem. In this way, we correct for the low value of the small-scale velocity dispersion characteristic of PM simulations. The resulting galaxy catalogue has a wide assortment of galaxy groups and clusters, but it undersamples field galaxies.

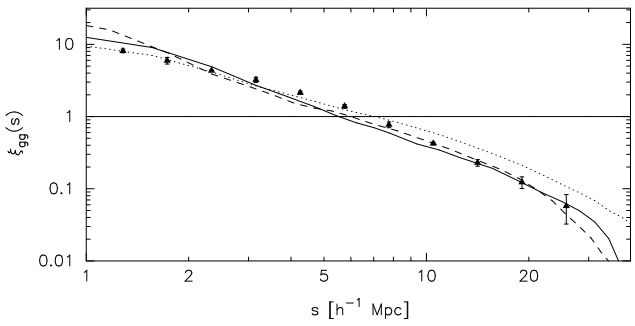

Figure 5. Comparison with theory at small-to-intermediate scales. The *filled triangles* are as in Fig. 1; the *solid line* denotes the $\xi_{\rm gg}(s)$ from the SCDM model, the *dashed line* denotes the $\xi_{\rm gg}(s)$ from the ΛCDM model, and the *dotted line* denotes the $\xi_{\rm gg}(s)$ from the BSI model.

In Figure 5, we compare the redshift-space autocorrelation functions of these simulated galaxy catalogues with the results from the LCRS. All three models well represent the observations. In particular, over the range $1 - 30h^{-1}$ Mpc, we obtain a $\xi_{\rm gg}(s)$ with the quite gentle slope of $\gamma \simeq -1.5$, comparable to that of the observed sample. Even so, we note that the small-scale peculiar velocities of the galaxy tracers in the SCDM simulation are higher than in either of the other two models. Therefore, the redshift-space distortions in the LCRS $\xi_{\rm gg}(s)$ promise to be a strong discriminating test of dark matter models (Lin et al. 1996b).

Looking more closely at the data we see that both the ΛCDM and the BSI autocorrelation functions show, on some scales, excess clustering relative to that of the LCRS – at small scales for the ΛCDM model and in the linear regime [$\xi_{\rm gg}(s) < 1$] for BSI. Both effects are influenced by the procedure of the galaxy selection, i.e., by the effective biasing of dark and luminous matter. We can thus conclude that the high quality of the LCRS $\xi_{\rm gg}(s)$ is a sensitive tool for verifying the modelling of this physically complex process, which could only be done crudely in our present simulations.

4 CONCLUSIONS

We have presented a detailed study of the LCRS redshift-space galaxy-galaxy autocorrelation function, $\xi_{\rm gg}(s)$. We found that the observed LCRS $\xi_{\rm gg}(s)$ can be approximated by a power law with slope $\gamma = -1.52 \pm 0.03$ and correlation length $s_0 = 6.28 \pm 0.27h^{-1}$ Mpc for separations $2.0h^{-1}$ Mpc $< s < 16.4h^{-1}$ Mpc, and that $\xi_{\rm gg}(s)$ first drops below zero at $s \sim 30 - 40h^{-1}$ Mpc. For $s \gtrsim 50h^{-1}$ Mpc, $\xi_{\rm gg}(s)$ fluctuates closely about zero, indicating that the galaxy distribution is quite homogeneous on these scales. Although possible secondary maxima, of amplitude $\delta\xi_{\rm gg} \approx 0.01 \pm 0.01$, are observed at $\sim 100h^{-1}$ Mpc and $\sim 200h^{-1}$ Mpc, their true significance is still under investigation.

Two selection criteria peculiar to fibre-optic redshift surveys – field-to-field variations in the rate of galaxy sampling and a limit to the observation of close galaxy pairs due to fibre-positioning constraints – were found, on most scales ($s \gtrsim 1h^{-1}$ Mpc), to have little or no effect on the measurement of the observed $\xi_{\rm gg}(s)$. On the smallest scales ($s \lesssim 1h^{-1}$ Mpc), the 55 arcsec fibre separation limit increasingly dampens the magnitude of the observed $\xi_{\rm gg}(s)$, by about 5 per cent at $s \approx 1h^{-1}$ Mpc to $10 - 20$ per cent at $s \approx 0.3h^{-1}$ Mpc to perhaps $\gtrsim 50$ per cent for $s \lesssim 0.15h^{-1}$ Mpc.

Finally, the observed LCRS $\xi_{\rm gg}(s)$ was compared with those from numerical simulations of the SCDM, ΛCDM, and BSI models. Although all of the model autocorrelation functions fit the observations reasonably well, we anticipate that the redshift-space distortions in the LCRS $\xi_{\rm gg}(s)$ will prove to be an even stronger test of the models. Furthermore, we conclude that, due to its high quality, the LCRS $\xi_{\rm gg}(s)$ provides a sensitive means for discriminating among the galaxy identification procedures of N-body simulations.

ACKNOWLEDGMENTS

The Las Campanas Redshift Survey has been supported by NSF grants AST 87-17207, AST 89-21326, and AST 92-20460. HL also acknowledges support from NASA grant NGT-51093. Thanks also to Dr. C. Heller (Göttingen) and to the anonymous referee for their respective suggestions at the inception and the completion of this work.

REFERENCES

Davis M., Peebles P. J. E., 1983, ApJ, 267, 465
Doroshkevich A. G., Tucker D. L., Oemler A. Jr., Kirshner R. P., Lin H., Shectman S. A., Landy S. D., Fong R., 1996, MNRAS, in press
Einasto J. et al., 1997, in preparation
Gottlöber S., Müller V., Starobinsky A. A., 1991, Phys. Rev. D, D43, 2510
Gottlöber S., Mücket J. P., Starobinsky A. A., 1994, ApJ, 434, 417
Groth E. J., Peebles P. J. E., 1977, ApJ, 217, 385
Hamilton A. J. S., 1993, ApJ, 417, 19
Kaiser N., Peacock J. A., 1991, ApJ, 379, 482
Kates R., Müller V., Gottlöber S., Mücket J. P., Retzlaff J., 1995, MNRAS, 277, 1254
Landy S. D., Szalay A. S., 1993, ApJ, 412, 64
Landy S. D., Shectman S. A., Lin H., Kirshner R. P., Oemler A., Tucker D. L., 1996, ApJ, 456, L1
Lin H., Kirshner R. P., Shectman S. A., Landy S. D., Oemler A., Tucker D. L., Schechter P. L., 1996a, ApJ, 464, 60
Lin H. et al., 1996b, in preparation
Lineweaver C. H., Tenorio L., Smoot G. F., Keegstra P., Banday A. J., Lubin P., 1996, ApJ, 470, 38
Ling E. N., Frenk C. S., Barrow J. D., 1986, MNRAS, 223, 21P.
Loveday J., Efstathiou G., Maddox S. J., Peterson B. A., 1996, ApJ, in press
Maddox S. J., Sutherland W. J., Efstathiou G., Loveday J., 1990b, MNRAS, 243, 692
Park C., Vogeley M. S., Geller M. J., Huchra J. P., 1994, ApJ, 431, 569
Shectman S. A., Landy S. D., Oemler A., Tucker D. L., Lin H., Kirshner R. P., Schechter P. L., 1996, ApJ, 470, 172

This paper has been produced using the Royal Astronomical Society/Blackwell Science LaTeX style file.